Generating Differentially Targeted Amyloid-β Specific Intrabodies as a Passive Vaccination Strategy for Alzheimer's Disease

Kelly L Sudol[1], Michael A Mastrangelo[1], Wade C Narrow[1], Maria E Frazer[1], Yona R Levites[2], Todd E Golde[2], Howard J Federoff[1,3,*] and William J Bowers[1,3]

[1]*Center for Neural Development and Disease, University of Rochester Medical Center, Rochester, New York, USA;* [2]*Department of Neuroscience, Mayo Clinic Jacksonville, Jacksonville, Florida, USA;* [3]*Departments of Neurology, University of Rochester Medical Center, Rochester, New York, USA*

Amyloid-β (Aβ) has been identified as a key component in Alzheimer's disease (AD). Significant *in vitro* and human pathological data suggest that intraneuronal accumulation of Aβ peptides plays an early role in the neurodegenerative cascade. We hypothesized that targeting an antibody-based therapeutic to specifically abrogate intracellular Aβ accumulation could prevent or slow disease onset. Aβ42-specific intracellular antibodies (intrabodies) with and without an intracellular trafficking signal were engineered from a previously characterized single-chain variable fragment (scFv) antibody. The intrabodies, one with an endoplasmic reticulum (ER) targeting signal and one devoid of a targeting sequence, were assessed in cells harboring a doxycycline (Dox)-regulated mutant human amyloid precursor protein Swedish mutant (hAPP^{swe}) transcription unit for their abilities to prevent Aβ peptide egress. Adeno-associated virus (AAV) vectors expressing the engineered intrabodies were administered to young adult 3xTg-AD mice, a model that develops amyloid and Tau pathologies, prior to the initial appearance of intraneuronal Aβ. Chronic expression of the ER-targeted intrabody (IB) led to partial clearance of Aβ42 deposits and interestingly, in reduced staining for a pathologic phospho-Tau epitope (Thr231). This approach may provide insights into the functional relevance of intraneuronal Aβ accumulation in early AD and potentially lead to the development of new therapeutics.

Received 5 January 2009; accepted 6 July 2009; published online 28 July 2009. doi:10.1038/mt.2009.174

INTRODUCTION

The accumulation of intraneuronal amyloid-β (Aβ occurs during initial stages of the Alzheimer's disease (AD) pathophysiologic cascade, yet this disease process remains relatively understudied as compared to classic amyloid plaque and neurofibrillary tangle pathologies. Significant *in vitro* and human pathological data suggest that intraneuronal Aβ peptides play an early triggering role in AD-related neurodegeneration. Masters *et al.* first reported marked staining of intraneuronal Aβ in pyramidal neurons of the hippocampus and entorhinal cortices of AD patients.[1] More recently, intracellular Aβ staining was detected prior to the appearance of paired helical filament-positive structures, further indicating that intraneuronal Aβ is one of the earliest documented AD-related changes. This alteration has also been suggested by Chui *et al.* to strongly correlate with cell damage and apoptotic cell death in AD patients.[2] Similar observations have been made in mouse AD models that neuronally overexpress Aβ peptides and in primary neuronal cultures transduced with viral vectors expressing hAPP.[3,4] Moreover, familial AD mutations in amyloid precursor protein (APP) lead to different profiles of intracellular Aβ accumulation, where the Swedish APP mutation results in a two- to threefold increase in intracellular Aβ levels as compared to cells expressing the wild-type *hAPP* gene.[5]

Increased oxidative stress, another early event in the AD pathologic cascade, exhibits a mechanistic connection with intracellular Aβ. Experimental application of an oxidative stressor, such as H_2O_2, to cells expressing hAPP results in enhanced intracellular Aβ levels and a concomitant decrease in full-length APP and carboxy-terminal fragments. In this prior study, *APP* gene expression was unchanged, suggesting that oxidative stress fosters intracellular Aβ peptide generation via alteration of APP proteolytic processing.[6] These data, in aggregate, point to intracellular Aβ accumulation as being not only a sentinel cellular process, but also a potentially viable therapeutic target.

To address the latter, we engineered a previously characterized Aβ-specific single-chain variable fragment (scFv) antibody[7] to specifically and efficiently abrogate the downstream pathologic effects of intracellular Aβ accumulation. ScFvs are composed of the minimal antibody-binding site formed by noncovalent association of the V_H and V_L variable domains joined by a flexible polypeptide linker (reviewed by ref. 8). Further antibody engineering makes it possible to manipulate the genes encoding scFvs for antibody-binding site expression within mammalian cells, whereas in-frame fusion of the *scFv* gene to intracellular targeting signals facilitates specific

[*]***Current address:*** *Office of the Executive Vice President for Health Sciences, Georgetown University Medical Center, Washington, DC, USA*
Correspondence: *William J Bowers, Department of Neurology, Center for Neural Development and Disease, University of Rochester Medical Center, 601 Elmwood Avenue, Box 645, Rochester, New York 14642, USA. E-mail: william_bowers@urmc.rochester.edu*

subcellular localization.[9,10] These intracellular antibodies, termed intrabodies, are capable of modulating target protein function by blocking or stabilizing macromolecular interactions; by modulating enzyme function through substrate sequestration, active site occlusion or active/inactive conformation stabilization; and/or by diverting proteins to alternative intracellular compartments (reviewed by refs. 11 and 12). In the present study, Aβ-specific intrabodies with differing intracellular trafficking characteristics were engineered into recombinant adeno-associated virus (rAAV) vectors. Focal stereotactic infusion of a rAAV vector expressing an endoplasmic reticulum (ER)-targeted anti-Aβ scFv into the hippocampi of young adult triple-transgenic AD (3xTg-AD) mice resulted in significant suppression of amyloid and Tau pathologies, indicating specific subcellular targeting of these promising therapeutics has the potential to disrupt downstream intraneuronal Aβ-associated pathological processes.

RESULTS

Creation and immunocytochemical analysis of a doxycycline-inducibile hAPP^{swe}-expressing stable cell line

To facilitate the analysis of anti-Aβ42 intrabody (IB) expression and subcellular localization *in vitro*, a stably transfected human amyloid precursor protein Swedish mutant (hAPP^{swe}) cell line was generated. Of note, eukaryotic cells exhibit evidence of toxicity when exposed to specific forms of proteolytically derived peptides of hAPP.[13] Hence, we utilized a previously described doxycycline (Dox)-regulated pBIG2i vector system to strictly control hAPP^{swe} expression and avoid transgene-related toxicity during generation of stably transfected clonal cell lines.[14] Following addition of the tetracycline homologue Dox, expression of the chimeric reverse tetracycline transactivator is feed-forward-activated via a tetracycline operator-controlled synthetic thymidine kinase promoter, whereas a synthetic cytomegalovirus (CMV) promoter is simultaneously upregulated to drive expression of the hAPP^{swe} transgene and the downstream reporter gene, enhanced green fluorescent protein (eGFP), via an internal ribosomal entry site. This construct, designated pBIG2i (hAPP^{swe}) and schematically illustrated in **Figure 1a**, was transfected into baby hamster kidney (BHK) cells and placed under hygromycin selection (600 μg/ml). Positive BHK-hAPP^{swe} clones were expanded and coimmunocytochemistry was performed for eGFP and hAPP^{swe}/Aβ (using the 6E10 monoclonal antibody) on cells incubated in the absence or presence of 0.5 or 2 μg/ml Dox. Cells were visualized using phase contrast and multicolor fluorescence microscopy. Neither eGFP nor hAPP^{swe}/Aβ proteins were detectable in the absence of Dox (**Figure 1b–e**). Robust expression of both eGFP and hAPP^{swe}/Aβ was apparent when BHK-hAPP^{swe} cells were incubated in the presence of 0.5 and 2 μg/ml Dox (**Figure 1f–m**). Co-expression of the two transgenes was significant, but there appeared to be a minor subset of cells that exhibited preferential expression of eGFP or hAPP^{swe}.

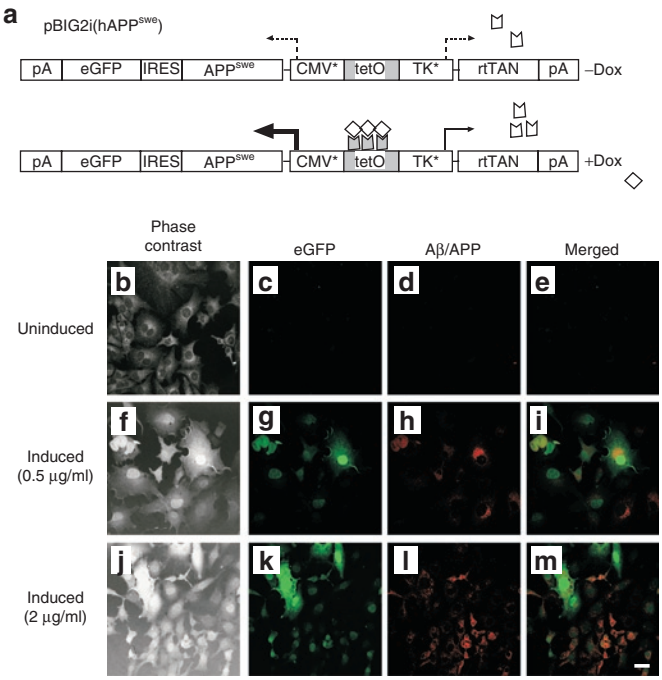

Figure 1 Generation of a doxycycline-inducible APP^{swe} stable cell line for characterization of Aβ42-specific intrabodies. (**a**) To generate a clonal cell line that conditionally expresses the human amyloid precursor protein Swedish mutant (hAPP^{swe}), the *hAPP^{swe}* gene was inserted into an autoregulated, bidirectional expression vector (pBIG2i[14]). Following addition of the tetracycline homologue doxycycline (Dox), expression of the chimeric reverse tetracycline transactivator is autoactivated via a Tet operator-controlled synthetic thymidine kinase (TK*) promoter, while a synthetic CMV promoter (CMV*) is simultaneously upregulated to drive expression of the hAPP^{swe} transgene and the downstream reporter gene, enhanced green fluorescent protein (eGFP), via an internal ribosomal entry site. This construct, designated pBIG2i(hAPP^{swe}), was transfected into baby hamster kidney (BHK) cells and placed under hygromycin selection (600 μg/ml). Positive BHK-hAPP^{swe} clones were expanded and coimmunocytochemistry was performed for eGFP and hAPP/amyloid-β (Aβ) on cells incubated in the absence (**b**–**e**) or presence of 0.5 μg/ml Dox (**f**–**i**) or 2 μg/ml Dox (**j**–**m**). Cells were visualized using phase contrast (**b**,**f**,**j**) and fluorescence microscopy. Green fluorescence depicts expression from the eGFP reporter gene (**c**,**g**,**k**) and red fluorescence signifies hAPP/Aβ expression (**d**,**h**,**l**). Co-registered staining is indicated in the merged images as yellow (**e**,**i**,**m**). Bar in m = 10 μm. Aβ, amyloid-β.

Engineering and *in vitro* testing of anti-Aβ42 IB-expressing rAAV vectors

Biosynthesis and post-translation modification of APP involves subcellular trafficking through the secretory pathway of the cell, initiating within the ER.[15] Here, APP undergoes a number of proteolytic processing events that are mediated by the α-secretase, which is a component of the nonamyloidogenic pathway, or the β- and γ-secretase complexes, which liberate pathogenic Aβ peptides as a result of the amyloidogenic processing pathway.[16] Available evidence suggests that when α-secretase cleaves the APP molecule this precludes the pathological generation through β-secretase activity of Aβ fragments 1–40 and 1–42.[17–20] Under circumstances where β-secretase cleavage is enhanced or α-secretase cleavage is diminished, pathological Aβ accumulation is augmented. Derivation of an anti-Aβ therapeutic that could encounter and undermine the pathogenic activity of Aβ at the point of its initial generation could significantly impact disease progression. To this end, we engineered a previously obtained single-chain antibody that specifically binds to the highly fibrillogenic Aβ42 peptide[7] into an "IB" to be differentially trafficked within an expressing neuron.

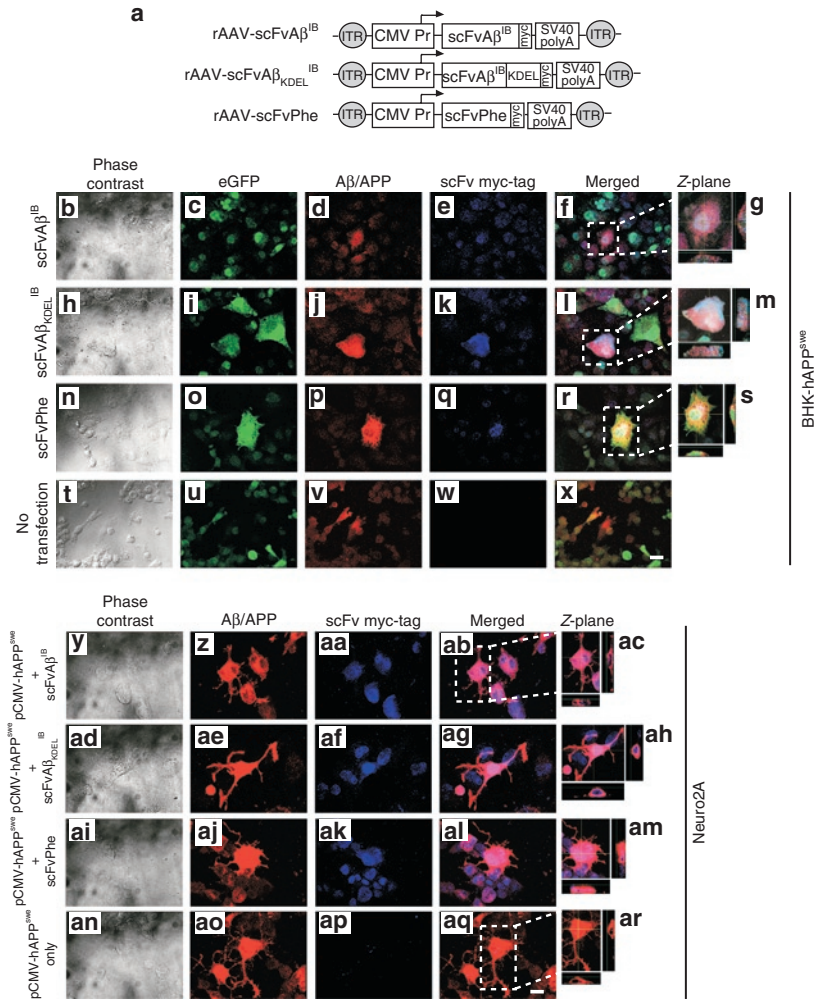

Figure 2 Colocalization of anti-Aβ42 intrabodies with hAPP^{swe}/Aβ *in vitro*. (**a**) Two recombinant adeno-associated virus (rAAV) vectors were constructed: one expressing an Aβ42-specific intrabody sequence with a c-*myc* epitope tag at the C-terminus to facilitate immunocytochemical detection (rAAV-scFvAβ^{IB}), and a second expressing the same c-*myc* tagged intrabody but with an endoplasmic reticulum targeting signal (KDEL) inserted in-frame between the intrabody coding sequence and c-*myc* epitope (rAAV-scFvAβ$_{KDEL}{}^{IB}$). The individual transgenes were placed under the transcriptional control of the human cytomegalovirus (CMV) promoter. A polyadenylation signal from SV40 was included at the 3′ end of the transcription unit, which in total was flanked by AAV inverted terminal repeat sequences. A rAAV vector expressing a phenobarbital-specific scFv that had been described previously was used as a negative control for a subset of *in vitro* studies.[45] The rAAV-scFvAβ^{IB} (**b**–**g**), rAAV-scFvAβ$_{KDEL}{}^{IB}$ (**h**–**m**), and rAAV-scFvPhe (**n**–**s**) plasmids were transiently transfected into the baby hamster kidney (BHK)-human amyloid precursor protein Swedish mutant (hAPP^{swe}) cells incubated in the presence of 2 µg/ml doxycycline (Dox), whereas nontransfected, Dox-treated BHK-hAPP^{swe} cells were used as negative controls (**t**–**x**). Forty-eight hours post-transfection, coimmunocytochemistry was performed for eGFP (green; **c**,**i**,**o**,**u**), hAPP/Aβ (red; **d**,**j**,**p**,**v**), and the c-*myc* epitope tag (blue; **e**,**k**,**q**,**w**). Images were obtained by confocal fluorescence microscopy at ×40 original magnification. Co-registered green/red/blue staining is indicated in the merged images as white (**f**,**g**,**l**,**m**,**r**,**s**,**x**). Co-registered green/red staining is indicated in the merged images as yellow. Panels **g**,**m**, and **s** represent *Z*-plane images of regions in **f**,**l**, and **r** demarcated with a white dotted box. The rAAV-scFvAβ^{IB} (**y**–**ac**), rAAV-scFvAβ$_{KDEL}{}^{IB}$ (**ad**–**ah**), and rAAV-scFvPhe (**ai**–**am**) plasmids were also transiently co-transfected with a plasmid expressing hAPP^{swe} into Neuro2A cells with, while Neuro2A cells transfected with only pCMV-hAPP^{swe} were used as controls (**an**–**ar**). Forty-eight hours post-transfection, coimmunocytochemistry was performed for hAPP/Aβ (red; **z**,**ae**,**aj**,**ao**) and the c-*myc* epitope tag (blue; **aa**,**af**,**ak**,**ap**). Images were obtained by confocal fluorescence microscopy at ×40 original magnification. Co-registered red/blue staining is indicated in the merged images as pink (**ab**,**ac**,**ag**,**ah**,**al**,**am**). Panels **ac**,**ah**,**am**, and **ar** represent *Z*-plane images of regions in **f**,**l**, and **r**. Bars in **x** and **aq** = 10 µm. scFv, single-chain variable fragment; Aβ, amyloid-β; IB, intrabody.

The original antibody, termed Aβ42.2, effectively prevented Aβ deposition when it was administered passively to amyloidogenic mice prior to amyloid formation.[7] The Aβ42.2 monoclonal antibody, was subsequently converted into a single-chain antibody fragment, and was extensively characterized.[7] The resultant scFv, ScFv42.2, retained its selectivity for Aβ42, as was demonstrated by pull-down with Aβ fibrils and by enzyme-linked immunosorbent assay (ELISA). When expressed intracranially via adeno-associated virus (AAV) injection into the cerebral ventricles of newborn mice, scFv42.2 prevented amyloid formation in CRND8 mice.

In the present study, two rAAV vectors were constructed (**Figure 2a**): one expressing an Aβ42-specific IB sequence with a c-*myc* epitope tag at the C-terminus to facilitate immunocytochemical detection (rAAV-scFvAβ^{IB}), and a second expressing the same c-*myc* tagged IB but with an ER-targeting signal (lysine-aspartic acid-glutamic acid-leucine (KDEL) inserted in-frame

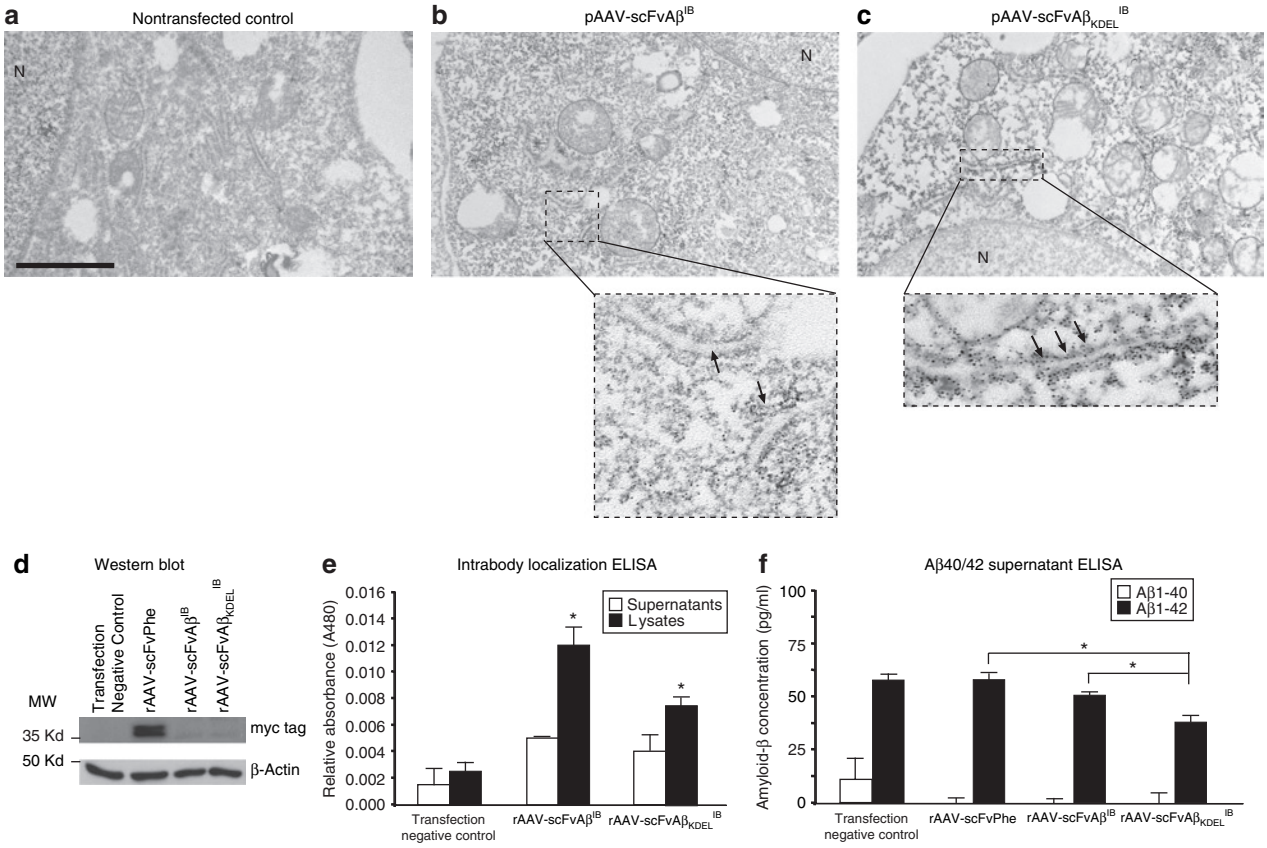

Figure 3 The engineered intrabody constructs maintain Aß42-binding activity, block egress of Aß42, and KDEL-targeted anti-Aß42 intrabody selectively localizes to endoplasmic reticulum ultrastructures within transiently transfected cells. To determine the subcellular localization of the individual intrabodies by immuno-electron microscopy, nontransfected baby hamster kidney (BHK) cells were used as negative controls (**a**) and the rAAV-scFvAβIB (**b**) and rAAV-scFvAβKDEL^{IB} plasmids (**c**) harboring the anti-Aβ42 intrabody expression cassettes were transiently transfected into BHK cells. Forty-eight hours post-transfection, cell monolayers were fixed and processed for immuno-electron microscopy using a c-*myc* epitope-specific antibody for detection of the engineered intrabodies. "*N*" designates the nucleus of the cell. The areas on the ×10,000 photomicrograph demarcated by the dotted boxes were visualized at ×45,000 and included in the respective insets. Arrows point to endoplasmic reticulum ultrastructures. Bar in **a** = 2,000 nm. (**d**) The rAAV-scFvAβ^{IB} and rAAV-scFvAβKDELIB plasmids, as well as the rAAV-scFvPhe control plasmid, were transiently transfected into BHK cells, and 48 hours later, cell lysates were generated and western blot analysis was performed using an anti-*myc* tag antibody to detect the engineered scFv proteins and an anti-β-actin antibody to assess protein loading. (**e**) Separately, the rAAV-scFvAβ^{IB} and rAAV-scFvAβKDEL^{IB} plasmids were transiently transfected into BHK cells (*N* = 4). After 48 hours, supernatants (white bars) and cell lysates (black bars) were analyzed by enzyme-linked immunosorbent assay (ELISA) to confirm the intrabodies maintained their ability to bind Aβ42 peptide coated onto microtiter plates. Nontransfected cell supernatants and lysates were used as negative controls. Error bars indicate standard deviation. "*"Indicates $P < 0.05$ as determined by analysis of variance (ANOVA). (**f**) The rAAV-scFvAβ^{IB} and rAAV-scFvAβKDEL^{IB} plasmids, as well as the rAAV-scFvPhe control plasmid, were transiently transfected into Dox-treated BHK-hAPPswe cells, and 48 hours later, culture supernatants were isolated and ELISA analyses were performed to measure human Aβ40 (white bars) and Aβ42 (black bars) release from the BHK-hAPPswe cells (*N* = 4). Nontransfected cell supernatants were used as negative controls. Error bars indicate standard deviation. "*"indicates $P < 0.05$ as determined by ANOVA. scFv, single-chain variable fragment; Aβ, amyloid-β; IB, intrabody; KDEL, lysine-asparticacid-glutanicacid-leucine.

between the IB coding sequence and c-*myc* epitope (rAAV-scFvAβ$_{KDEL}^{IB}$). The individual transgenes were placed under the transcriptional control of the human CMV promoter. A SV40-derived polyadenylation signal was included at the 3′ end of the transcription unit, which in total was flanked by AAV genome-derived inverted terminal repeat sequences. The resulting rAAV-scFvAβ^{IB} and rAAV-scFvAβ$_{KDEL}^{IB}$ plasmids were transiently transfected into BHK-hAPP^{swe} cells incubated in the presence of 2 μg/ml Dox, whereas nontransfected, Dox-treated BHK-hAPP^{swe} cells were used as negative controls. Forty-eight hours post-transfection, coimmunocytochemistry was performed for eGFP, hAPP/Aβ, and the c-*myc* epitope tag, and images were obtained by confocal fluorescence microscopy (**Figure 2b–x**). In parallel, the IB plasmids were co-transfected individually with a hAAP^{swe}-expressing plasmid (pCMV-hAPP^{swe}) into the neuroblastoma-derived cell line, Neuro2A (**Figure 2y–ar**). Both anti-Aβ42 intrabodies were readily detectable within transfected BHK-hAPP^{swe} and Neuro2A cells by immunocytochemistry. Moreover, the extent of colocalization of anti-Aβ42 IB and hAPP/Aβ staining was substantial, suggesting that each was residing within similar subcellular compartments.

To more definitively assess the subcellular localization of each IB, immuno-electron microscopy was performed. The rAAV-scFvAβ^{IB} and rAAV-scFvAβ$_{KDEL}^{IB}$ plasmids were transiently transfected into BHK cells, whereas nontransfected BHK cells were used as negative controls. Forty-eight hours post-transfection, cell monolayers were fixed and processed for immuno-electron microscopy using a c-*myc* epitope-specific antibody for detection of the engineered intrabodies. BHK cells expressing rAAV-scFvAβ$_{KDEL}^{IB}$

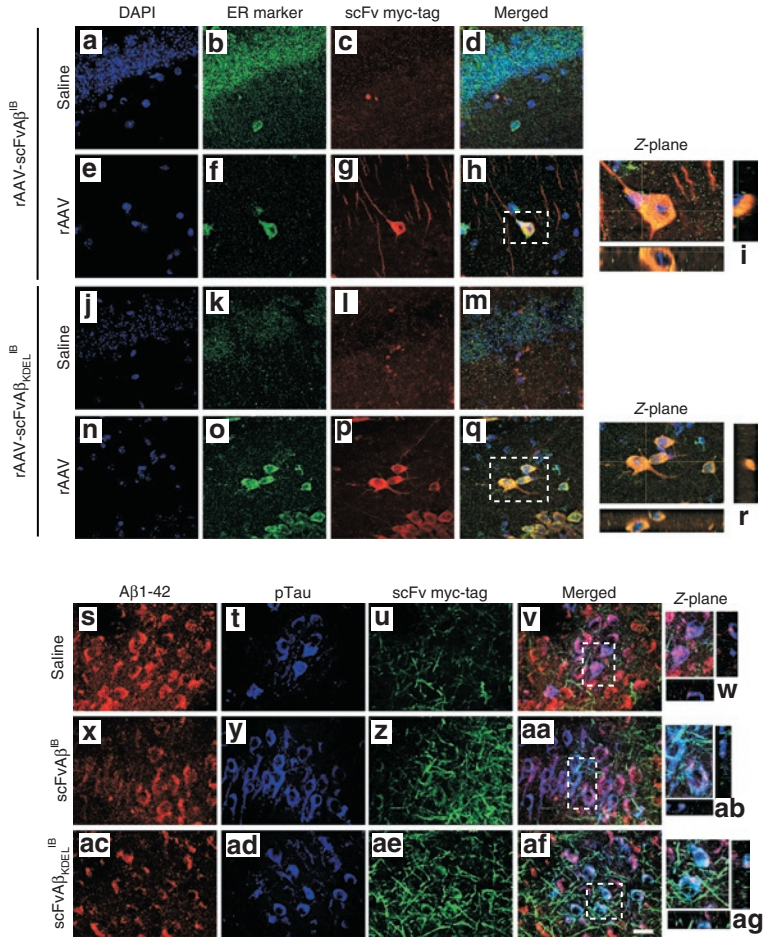

Figure 4 AAV vector–mediated expression of the Aβ-specific intrabodies in 3xTg-AD mice reveals the intrabodies alter general patterns of cell-associated Aβ42. Two month-old 3xTg-AD mice were unilaterally injected in the CA1 region of the hippocampus with saline (**a**–**d** and **j**–**m**), recombinant adeno-associated virus (rAAV)-scFvAβ^{IB} (**e**–**i**) and rAAV-scFvAβ$_{KDEL}{}^{IB}$ (**n**–**r**). Nine months postinjection animals were killed and brain sections were processed for coimmunocytochemistry with the following: 4′,6-diamidino-2-phenylindole (blue; **a**,**e**,**j**,**n**), endoplasmic reticulum-specific antibody (green; **b**,**f**,**k**,**o**) and c-*myc* epitope tag-specific antibody (red; **c**,**g**,**l**,**p**). Co-registered staining is indicated in the merged images as yellow (**d**,**h**,**m**,**q**). Panels **i** and **r** represent digitally magnified images, which illustrate a cross section through the *Z*-plane obtained with confocal microscopy. All images were obtained at ×100 original magnification. Additional brain sections from these rAAV vector-injected 3xTg-AD mice were processed for fluorescence coimmunocytochemistry with the following: Aβ42-specific antibody (red; **s**,**x**,**ac**), phospho-Tau (AT180)-specific antibody (blue; **t**,**y**,**ad**) and c-*myc* epitope tag-specific antibody (green; **u**,**z**,**ae**). Co-registered staining for all markers is indicated in the merged images as white or for Aβ42 and phospho-Tau as purple (**v**,**w**,**aa**,**ab**,**af**,**ag**). Panels **w**,**ab**, and **ag** represent digitally magnified images, which illustrate a cross section through the *Z*-plane obtained with confocal microscopy. All images were obtained at ×100 original magnification. scFv, single-chain variable fragment; Aβ, amyloid-β; IB, intrabody.

exhibited a qualitative enhancement in electron-dense signal localizing to ER-related ultrastructures (indicated by black arrows) as compared to rAAV-scFvAβ^{IB}-expressing cells and nontransfected control cells (**Figure 3a–c**). The relative intensities of ER-associated signal could not be attributed to differential levels of IB expression as quantitative real-time reverse transcriptase PCR analysis of transfected cultures indicated that transcripts encoding each IB were expressed at similar levels (data not shown).

To assess relative steady-state levels of the intrabodies at 48 hours after transfection of BHK cells, western blotting was performed. Incubation of blots with a c-*myc* epitope-specific antibody led to the detection of low, but similar, levels of each IB at the expected size of 36 kd (**Figure 3d**). To ensure that molecular engineering did not lead to ablation of target antigen recognition, the Aβ42-binding activity of each IB was tested by ELISA. BHK cells were transiently transfected with the rAAV-scFvAβ^{IB} and rAAV-scFvAβ$_{KDEL}{}^{IB}$ plasmids, and 48 hours later supernatants and cell lysates were collected and applied to 96-well plates coated with Aβ42 peptide. Nontransfected cell supernatants and lysates were used as negative controls. IB binding to the Aβ42-coated microtiter plates was detectable in lysates generated from cells transfected with rAAV-scFvAβ^{IB} and rAAV-scFvAβ$_{KDEL}{}^{IB}$ plasmids. Supernatants from these cultures harbored significantly less Aβ42 binding activity, suggesting that both anti-Aβ42 intrabodies were retained within the transfected cell (**Figure 3e**). We separately transfected Dox-induced BHK-APP^{swe} cells with rAAV plasmids encoding the intrabodies or rAAV-scFvPhe control plasmid and analyzed culture supernatants for Aβ40 and Aβ42 by ELISA. Only cultures transfected with the ER-targeted anti-Aβ42 IB construct exhibited a statistically significant diminution in secreted Aβ42 (**Figure 3f**). Although culture

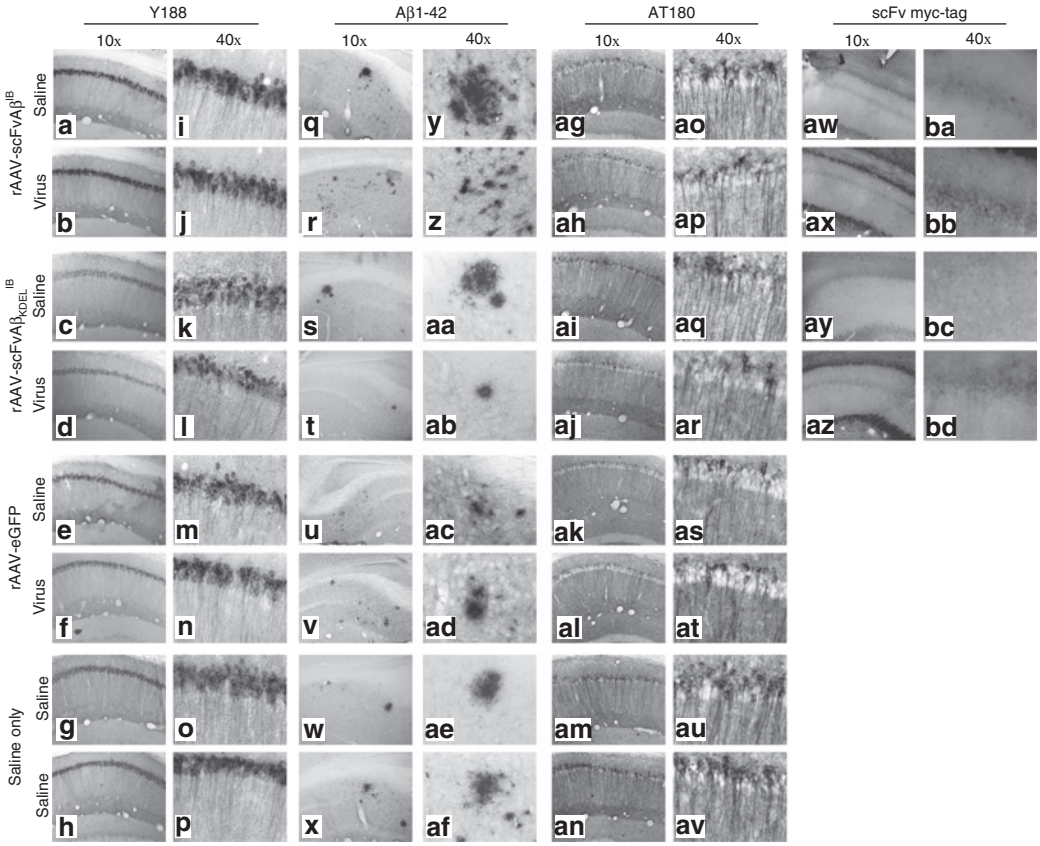

Figure 5 Qualitative effects of chronic anti-Aβ42 intrabody expression on AD-related pathological hallmarks. Two month-old 3xTg-Alzheimer's disease mice were unilaterally injected in the CA1 region of the hippocampus with saline, recombinant adeno-associated virus (rAAV)-enhanced green fluorescent protein, rAAV-scFvAβ^{IB} or rAAV-scFvAβ$_{KDEL}$^{IB}. Nine months postinjection animals were killed and 30-µm brain sections were processed for immunohistochemical analyses of hAPP transgene expression (Y188 antibody; **a**–**p**), extracellular Aβ 1–42 deposition (anti-Aβ42 antibody; **q**–**af**), hyperphosphorylated Tau (AT180 antibody; **ag**–**av**), and c-*myc* epitope tag-specific antibody (**aw**–**bd**). Of note, the images obtained for the c-*myc* epitope tag immunohistochemical analysis were obtained originally in color by fluorescence microscopy, converted to black-and-white, and subsequently inverted to provide comparable views to the other sections captured using conventional light microscopy following 3,3′-diaminobenzidine immunohistochemistry. Representative images of the infused hippocampus are displayed at ×10 (**a**–**h**,**q**–**x**,**ag**–**an**,**aw**–**az**) and ×40 original magnification (**i**–**p**,**y**–**af**,**ao**–**av**,**ba**–**bd**). scFv, single-chain variable fragment; Aβ, amyloid-β; IB, intrabody.

supernatants from cells transfected with the nontargeted IB showed a trending decrease in Aβ42 levels, this decrease did not reach statistical significance as compared to nontransfected or rAAV-scFvPhe transfected cultures. Due to the Dox-regulated expression of the Swedish APP mutant in these cells, only Aβ42 is detectable, whereas Aβ40 concentrations lie at baseline levels.

In vivo assessment of anti-Aβ42 intrabodies in the 3xTg-AD mouse model

To determine whether chronic Aβ42-specific IB expression *in vivo* could abrogate amyloid-related pathology, and whether subcellular targeting of the IB would influence its effectiveness in doing so, we subsequently packaged the rAAV-scFvAβ^{IB} and rAAV-scFvAβ$_{KDEL}$^{IB} plasmids into serotype 2 virions and delivered these constructs intrahippocampally to triple-transgenic AD mice (3xTg-AD). The 3xTg-AD mouse, created in the LaFerla laboratory, develops intracellular Aβ, amyloid plaques and neurofibrillary tangles in a progressive and age-related pattern.[21–23] Two month-old male 3xTg-AD mice were stereotactically infused with rAAV-scFvAβ^{IB}, rAAV-scFvAβ$_{KDEL}$^{IB}, or an eGFP-expressing rAAV vector control (rAAV-eGFP) unilaterally into the CA1 layer of the hippocampal formation (n = 6 per group). An equivalent volume of saline was identically infused into the contralateral hippocampus to serve as a no-vector control. Mice at this age exhibit neither pathological nor behavioral signs of AD.[23,24] Nine months post-transduction, animals were killed and brains were sectioned for further analyses. Coimmunocytochemistry for IB expression and GRP94, an ER-localized protein, and subsequent staining of cellular nuclei with 4′,6-diamidino-2-phenylindole revealed confocal co-registration of fluorescent signals for GRP94 and the rAAV vector-expressed intrabodies, but not with the nuclear stain (**Figure 4a–r**). We also performed triple immunocytochemistry for the c-*myc* epitope tag of the intrabodies, Aβ42 and phospho-Tau (as detected by the AT180 antibody) and used confocal microscopy to visualize the spatial relationship of IB expression and the accumulation of Aβ42 and phospho-Tau. The photomicrographs show, especially for the ER-targeted Aβ42 IB, the staining patterns/intensities for Aβ42 and phospho-Tau are altered in regions expressing the intrabodies (**Figure 4s-ag**). Unfortunately, the fluorescein isothiocyanate preconjugated primary antibody used to detect the c-*myc* epitope led to higher background signals in neuronal processes for this triple immunocytochemical assessment, but even given this technical

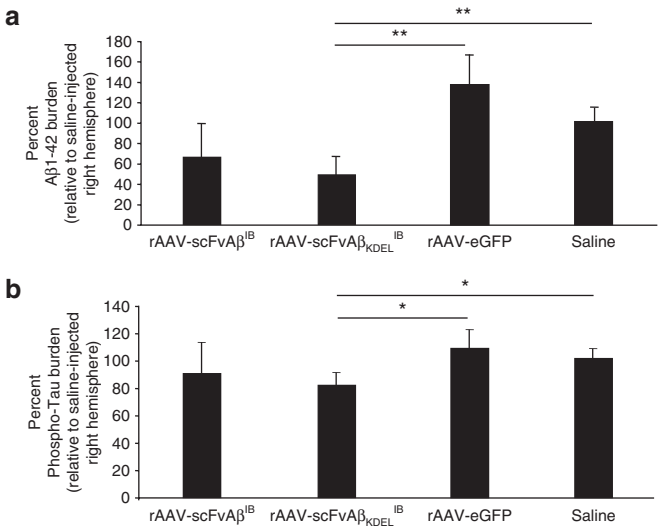

Figure 6 Recombinant adeno-associated virus (rAAV)-scFvAβ$_{KDEL}^{IB}$ delivery results in a quantitative reduction in immunoreactive Aβ42 plaque burden and phospho-Tau pathology. Coronal brain sections from 11 month-old 3xTg-Alzheimer's disease (AD) animals that were injected with rAAV-scFvAβ^{IB}, rAAV-scFvAβ$_{KDEL}^{IB}$, rAAV-enhanced green fluorescent protein, or saline were processed for immunohistochemistry with 3,3′-diaminobenzidine development, and two AD pathologic markers were quantified using the MCID Elite program. The percent of Aβ42 plaque burden relative to the saline-injected right hemisphere (**a**) was determined by enumerating all the immunoreactive plaque in consecutive coronal brain sections. The percent of phospho-Tau burden was calculated in a similar manner (**b**). Error bars indicate standard error of the mean. "*" equals $P < 0.05$ and "**" equals $P < 0.001$ as determined by Student's *t*-test. scFv, single-chain variable fragment; Aβ, amyloid-β; IB, intrabody.

caveat, relative proximity information relating to localization of IB, Aβ42 and phospho-Tau could be gleaned.

To determine the extent to which AAV-vectored Aβ42-specific IB expression altered the severity of AD-related amyloid and Tau pathologies in 3xTg-AD mice and whether differential subcellular targeting of the IB altered therapeutic outcome, we subsequently performed immunohistochemistry for hAPP, extracellular Aβ42, and phospho-Tau. Although the intrabodies were designed to be specific for Aβ42, it was possible that chronic expression *in vivo* could impact the accumulation of the hAPP^{swe} transgene product, which would suggest that the specificity of the intrabodies is not absolute. This potential caveat may prove disadvantageous therapeutically given APP plays a likely role in normal neuronal physiology and its untoward removal could lead to yet unknown deleterious consequences (reviewed by ref. 25). Immunohistochemical assessment using the hAPP-specific Y188 antibody indicated that chronic Aβ42-specific IB expression did not overtly alter the pattern or intensity of hAPP^{swe} staining within the transduced CA1 layer of the 3xTg-AD hippocampus (**Figure 5a–p**). Immunohistochemical staining of hippocampi from AAV vector-infused 3xTg-AD mice using the Aβ42-specific 12F4 monoclonal antibody and the phospho-Tau-specific AT180 antibody demonstrated that Aβ42-specific IB expression (cytoplasmically or ER-localized) qualitatively impacted amyloid and Tau pathologies when saline control hemispheres were compared to contralateral vector-injected hemispheres (**Figure 5q-av** and **Supplementary Figure S1**). Stereologic examination of vector-infused hippocampal regions revealed inter-treatment group quantitative differences in relation to the severity of extracellular Aβ42 deposition and appearance of a pathologically relevant phospho-Tau epitope (**Figure 6**). Although rAAV-scFvAβ^{IB}-treated mice collectively exhibited trending decreases in extracellular Aβ42 and phospho-Tau burden within their vector-injected hemispheres relative to saline-injected contralateral hippocampi, these differences did not reach statistical significance. Mice receiving rAAV-scFV$_{KDEL}^{IB}$ manifested statistically significant differences in both extracellular Aβ42 and intracellular phospho-Tau staining compared to controls. Negative control groups (rAAV-eGFP and saline-injected 3xTg-AD mice) did not exhibit notable differences in the severities of the AD-related pathologies analyzed. We do not believe that IB-mediated epitope masking accounts for the apparent diminution in extracellular Aβ42. If that were the case, it would not be expected *a priori* that the staining for the phospho-epitope of Tau at residue Thr231 using the AT180 antibody would have significantly decreased. Our findings further confirmed that therapeutic approaches designed to abrogate Aβ accumulation can influence Tau-related pathological outcomes in 3xTg-AD mice.[26–28]

DISCUSSION

The marked prevention of extracellular Aβ42 deposition and delay in appearance of a disease-related phospho-epitope of Tau in 3xTg-AD mice observed in the present study supports the feasibility of chronically expressed anti-Aβ intracellular scFv antibodies to interdict AD pathogenesis *in vivo*. Other investigators have pursued viral vector-based approaches to deliver scFvs as a means to target extracellular Aβ. Levites *et al.* compared three scFvs specific to three distinct linear epitopes: Aβ1–16, monomeric Aβ40, and monomeric Aβ42.[7] CRND8 AD mice were given intraventricular injections at P0 and killed 3–5 months later. At 3 months each scFv demonstrated a decrease in plaque load, a decrease in SDS-soluble Aβ40 and 42 levels, as well as promoted the efflux of Aβ-scFv complexes into the plasma. Fukuchi *et al.* used serotype 2 rAAV vectors to deliver scFvs that recognized tetrameric Aβ to the brains of Tg2576 AD mice.[29,30] A decrease in Aβ load was observed via immunohistochemistry in scFv-injected mice compared to phosphate buffered saline–infused control animals. Controversy does exist as to how scFvs promote the removal and/or degradation of target antigens from the extracellular space *in vivo* given their lack of an Fc segment, which is classically recognized by cognate receptors on brain microglia for facilitation of phagocytosis. However, despite the unknowns, these prior *in vivo* studies provide confidence that the general methods of viral vectored Aβ-specific scFvs are well-tolerated and effective in diminishing amyloid-related pathology in AD mouse models.

Perhaps most relevant to our approach to employ modified scFvs for intracellular Aβ targeting relates to the work from Lecerf *et al.*[31] and more recently by Paganetti *et al.*[32] and Lynch *et al.*[33] The former identified human scFv intrabodies capable of interacting *in situ* with huntingtin thereby reducing its ability to aggregate.[31] These scFvs were bound to the N-terminal residues of huntingtin and maintained the normally aggregated protein in a soluble complex that subsequently underwent normal protein turnover. Specificity of binding was further determined by fusing the antihuntingtin scFv with a nuclear localization signal

and the subsequent retargeting of soluble huntingtin to cell nuclei. Prevention of specific aggregate formation in cellular models of Huntington's disease suggested that intracellular scFvs may represent a viable therapy for this disease as well as other neurodegenerative diseases with abnormal protein processing/accumulation/aggregation such as Aβ in AD. To that end, Paganetti *et al.* demonstrated that intrabodies designed to bind to an epitope proximal to the β-secretase cleavage site of hAPP significantly blocked Aβ generation in a cell culture model.[32] In fact, these authors also found that ER targeting of the IB resulted in more efficient blocking of APP processing. More recently, Lynch *et al.* isolated and tested scFv-based intrabodies specific for the nonamyloid component of α-synuclein.[33] The authors demonstrated that an anti–nonamyloid component IB could redirect synuclein trafficking intracellularly and showed that a neural progenitor cell line stably expressing one of these intrabodies exhibited significantly decreased mutant synuclein aggregation.

Although 3xTg-AD mice receiving the ER-targeted anti-Aβ42 IB exhibited evidence of improved AD-related pathological status as compared to control animals, this strategy portends a number of potential caveats. The possibility exists that IB-mediated retention of Aβ42 intracellularly could lead to increased APP processing that would yield more of the fibrillogenic Aβ42 species.[34] This may result in enhanced intracellular aggregation and cellular dysfunction. Moreover, we are aware that high concentrations of IB/Aβ complexes intralumenally could inherently block normal cellular protein maturation, ultimately leading to cellular stress. Excessive aggregation could also lead to proteasomal activity inhibition.[35] In the present study, we did not observe overt loss of neurons within the transduced CA1 layer of the hippocampus. However, if such an outcome were to occur, a weaker promoter could be employed in the rAAV vector backbone that would lead to lower levels of IB expression, proteasome-targeting sequences could be appended to the intrabodies to facilitate degradation,[36] or even regulatable rAAV vectors could be engineered to finely control *IB* gene expression. A variety of regulated rAAV vector platforms have been developed and shown to be effective *in vivo*.[37,38]

Given the advances in brain-wide dissemination via convection-enhanced delivery of AAV vector particles, we believe that an IB-based approach has significant therapeutic merit in the future. Convection-enhanced delivery was first described by Bobo *et al.*[39] and has steadily gained acceptance for widespread distribution of small-molecule therapeutics and viral vectors within the brain.[40,41] This local infusion technique uses bulk flow to enable the delivery of small and large molecules to clinically significant volumes of targeted tissues, offering an improved volume of distribution (V_d) compared to simple diffusion. We envision at least panhippocampal diffusion of the IB-expressing AAV vector would be required as well as delivery to entorhinal cortex, which are regions affected earliest in AD. Moreover, AAV vectors have the ability to retrogradely migrate along axons, enabling dissemination to distal brain regions, if necessary and carefully monitored during infusion using advanced imaging techniques.[42]

Gaining an enhanced understanding of mechanisms relating to target antigen clearance and the subversive role of intracellular Aβ in disease pathophysiology, as well as devising approaches that will not significantly overburden a compromised proteasomal machinery within AD-afflicted neurons provide significant challenges. However, the growing literature detailing the successful implementation of IB-based therapeutics in preclinical models of neurodegenerative diseases and tumorigenesis presents ample justification for optimization of the platform to enhance its safety profile and for future development and testing in a clinical setting.

MATERIALS AND METHODS

Inducible human-APPswe expressing cell line. The gene encoding the Swedish mutant form of hAPP^{swe} was removed from its parental vector (kindly provided by William Van Nostrand) and cloned into the pBIG2i vector.[14] The pBIG2i(hAPP^{swe}) construct was stably transfected into BHK cells and placed under hygromycin selection (600 μg/ml). Expression of the *hAPP^{swe}* gene was induced with Dox (2 μg/ml or 0.5 μg/ml) and inducible hAPP^{swe} expression was subsequently confirmed by immunocytochemistry. Three separately generated cell clones were isolated and analyzed.

Single-chain intrabodies. PCR was used to amplify the anti-Aβ42 213scFv antibody sequence from the parental pSecTag construct (Invitrogen, Carlsbad, CA) to remove its artificial immunoglobulin-κ secretion signal (while retaining an endogenous leader peptide) and facilitate its cloning into a CMV immediate-early promoter-containing shuttle plasmid, pBSFBRmcs.[43] To complete the rAAV-scFvAβ_{KDEL}^{IB} vector, the intermediate plasmid was subsequently digested with AflIII and EcoRI and the following phosphorylated double-stranded linker encoding the KDEL ER-targeting sequence was ligated into the plasmid: sense strand—5′-CATGTAAGGACGAGCTGTGAG-3′ and antisense strand—5′-AATTCTCTCAGCTCGTCCTTA-3′. The CMV promoter-driven IB expression cassettes were excised out of the respective pBSFBRmcs intermediates with NotI and cloned into a NotI-cut pFBGR rAAV plasmid (kindly provided by R. Kotin). Each resultant rAAV plasmid was packaged into serotype 2 rAAV virions along with an eGFP encoding rAAV control vector, rAAV-eGFP, using a baculovirus-based method.[44] A previously described rAAV vector plasmid expressing a phenobarbital-specific scFv (scFvPhe) was used in a subset of *in vitro* studies as a negative control.[45]

In vitro *immunocytochemical assessment.* Dox-treated (2 μg/ml) or non-treated BHK-hAPP^{swe} cells were plated on glass cover slips and transiently transfected with the rAAV plasmids encoding the anti-Aβ42 intrabodies or scFvPhe control plasmid. Neuro2A cells were plated identically and transiently co-transfected with one of the scFv plasmids described above with pCMV-hAPP^{swe}, a plasmid that expresses the Swedish mutant of hAPP. The cells were stained for expression of the scFvs (anti-c-*myc*; Rockland Immunochemicals, Gilbertsville, PA) and expression of hAPP^{swe}/Aβ (6E10; Signet, Dedham, MA). The expression of eGFP was also noted. Confocal fluorescent images were obtained at 488, 568, and 647 nm.

Western blotting. Companion BHK-hAPP^{swe} cultures were plated in 6-well dishes, transiently transfected with 1.5 μg IB-expressing plasmids or rAAV-scFvPhe control plasmid per well, and lysates analyzed by western blotting using the 9E10 anti-myc epitope antibody (1:500, Sigma, St Louis, MO). An anti-β-actin antibody (1:3,000; Sigma) was used to re-probe blots to assess loading consistency. Blots were developed using the Perkin-Elmer Western Lightning Kit (Perkin-Elmer, Waltham, MA).

Maintenance of IB anti-Aβ42 binding activity assay. Companion BHK-hAPP^{swe} cultures were plated and transiently transfected with IB-expressing plasmids for ELISA-based assessment of their respective Aβ42 binding activities. Following transfection, cells were incubated for 48 hours at 37 °C. Supernatants were collected and lysates generated. Microtiter plates (Corning Life Sciences, Lowell, MA) were coated using 500 ng of Aβ42 peptide per well (Tocris Cookson, Ellisville, MO). Plates were washed followed by addition of a dilution series of cell supernatants or lysates in phosphate

buffered saline added in triplicate, or a positive control rabbit anti-Aβ antibody of (1:5,000, Chemicon International, Temecula, CA) to appropriate wells. Appropriate secondary antibodies were added (1:3,000; goat anti-c-*myc*, Novus Biologicals, Littleton, CO or 1:1,000; goat anti-rabbit, Jackson Laboratories, West Grove, PA) and plates were developed using 3,3′,5,5′,-tetramethyl benzidine (Sigma-Aldrich, St Louis, MO) and phosphate citrate buffer (Sigma-Aldrich). Plates were analyzed at an absorbance of 450 nm using a Bio-Rad Model 550 microplate reader (Bio-Rad, Hercules, CA).

Aβ40 and Aβ42 ELISA. Dox-treated BHK-hAPP^{swe} cultures (2 μg/ml) were plated in 24-well dishes, transiently transfected with 0.4 μg IB-expressing plasmids or rAAV-scFvPhe control plasmid per well, and 48 hours later culture supernatants were analyzed using ELISA kits specific for Aβ 40 and 42 according to manufacturer's instructions (Covance, Berkeley, CA).

Immuno-electron microscopy. BHK cells were plated into a 12-well tissue culture plate onto glass coverslips at a density of 1×10^5 cells/well. Cells were transfected the following day, and after a 24-hours incubation, cells were fixed, permeabilized, and incubated with blocking solution (1% bovine serum albumin, 2% normal horse serum, 0.1% fish gelatin, 0.01% Triton X-100). The primary mouse monoclonal 9E10 anti-c-*myc* (1:100, Sigma, St Louis, MO) and biotinylated goat anti-mouse secondary antibody (1:2,000, Vector Laboratories, Burlinghame, CA) were used. Coverslips were post-fixed with 2% glutaraldehyde, dehydrated and embedded in Epon in preparation for electron microscopy. Ultrathin sections were counterstained with uranyl acetate followed by lead citrate and examined using a Hitachi 7100 transmission electron microscope. Images for single-chain antibody localization were taken using a MegaView III digital camera and AnalySIS (Soft Imaging Systems, Lakewood, CO) software. Images were captured at ×10,000 and ×30,000 magnification.

Stereotactic vector infusions. rAAV vectors (3×10^9 transduction units) were stereotactically delivered into 2 month-old male and female 3xTg-AD mice ($n = 6$ per condition) in accordance with approved University of Rochester animal use guidelines as described previously.[43] At 11 months of age, vector-injected mice were killed and perfused with 4% paraformaldehyde.

Fluorescent immunocytochemistry. Paraformaldehyde-fixed brains removed, sectioned into 30-μm coronal sections using a sliding microtome, and processed for immunocytochemistry as previously described.[43] Brain sections were incubated overnight at 4 °C with primary antibodies specific for the ER marker GRP94 (rabbit anti-mouse, 1:500 dilution, Abcam) and the c-*myc* epitope tag incorporated into the IB sequences (mouse anti-c-*myc*, 1:1,000 dilution, 9E10, Sigma). Fluorescently labeled secondary antibodies (goat anti-rabbit Alexa 488 for GRP94 and goat anti-mouse Alexa 568 for c-*myc*, 1:2,500 dilution, Invitrogen, Carlsbad, CA) were subsequently used. Sections were washed and then histochemically stained with 4',6-diamidino-2-phenylindole. For AD-related protein colocalization analyses, the following primary antibodies were employed: rabbit anti-Aβ42 (1:1,000, Invitrogen), antihuman phosphorylated Tau AT180 (1:200, Pierce, Rockford, IL), and pre-fluorescein isothiocyanate conjugated 9E10 (1:1,000). The secondary antibodies Alexa 568 for anti-Aβ42 and Alexa 450 for phospho-Tau were then used. Imaging was performed using a Zeiss Scanning confocal microscope (Carl Zeiss, Minneapolis, MN).

3,3′-diaminobenzidine immunohistochemistry. The following antibodies were used at the designated working dilutions: anti-APP A4, corresponding to the NPXY motif of hAPP, (Clone Y188; 1:750, AbCam, Cambridge, MA); anti-Aβ 1-42 clone 12F4 reactive to the C-terminus of Aβ42 (1:1,000, Covance, Berkeley, CA) and antihuman phosphorylated Tau AT180, specific for hTau phosphorylated at the Thr231 residue (1:200, Pierce, Rockford, IL1:200). For Aβ peptide-specific detection, the sections were treated with 70% formic acid for 15 minutes. for epitope retrieval. The sections were further processed for immunohistochemistry as previously described.[23] Sections were viewed using an Olympus AX-70 microscope and motorized stage (Olympus, Center Valley, PA) and the MCID 6.0 Imaging software (Interfocus Imaging, Cambridge, UK).

Quantitation of staining intensities. Quantification of positively stained targets was performed as previously described.[46] Three consecutive images per tissue section (10 sections per mouse) were obtained at ×40 magnification in the CA1 region of the hippocampus using an Olympus AX-70 microscope equipped with a motorized stage (Olympus, Melville, NY). Sections corresponding to 2.5–2.9 mm posterior from Bregma were analyzed. Estimated target numbers were determined for each area using MCID 6.0 Elite Imaging Software (Interfocus Imaging, Cambridge, UK).

Statistical analyses. Data were analyzed by means of Student's *t*-test or analysis of variance, followed by post hoc comparison using Bonferroni's method in the GraphPad Prism v.4.0 (GraphPad Prism Software, San Diego, CA) data analysis software package. $P < 0.05$ was considered statistically significant.

SUPPLEMENTARY MATERIAL

Figure S1. Representative photomicrographs of AT180-stained 3xTg-AD mice receiving hippocampal infusions of rAAV-vectored intrabody constructs.

ACKNOWLEDGMENTS

The authors wish to thank Linda Callahan (University of Rochester) for immunohistochemistry and microscopy advice, Sarah Woods (University of Rochester) for stereological assessments, and Karen L. de Mesy Bentley (University of Rochester) for electron microscopy services and advice. Supported by NIH R01-AG020204 to HJF, and NIH R01-AG023593 and NIH R21-AG031878 to WJB.

REFERENCES

1. Masters, CL, Multhaup, G, Simms, G, Pottgiesser, J, Martins, RN and Beyreuther, K (1985). Neuronal origin of a cerebral amyloid: neurofibrillary tangles of Alzheimer's disease contain the same protein as the amyloid of plaque cores and blood vessels. *EMBO J* **4**: 2757–2763.
2. Chui, DH, Dobo, E, Makifuchi, T, Akiyama, H, Kawakatsu, S, Petit, A *et al.* (2001). Apoptotic neurons in Alzheimer's disease frequently show intracellular Abeta42 labeling. *J Alzheimers Dis* **3**: 231–239.
3. Kienlen-Campard, P, Miolet, S, Tasiaux, B and Octave, JN (2002). Intracellular amyloid-beta 1-42, but not extracellular soluble amyloid-beta peptides, induces neuronal apoptosis. *J Biol Chem* **277**: 15666–15670.
4. LaFerla, FM, Tinkle, BT, Bieberich, CJ, Haudenschild, CC and Jay, G (1995). The Alzheimer's A beta peptide induces neurodegeneration and apoptotic cell death in transgenic mice. *Nat Genet* **9**: 21–30.
5. Takeda, K, Araki, W and Tabira, T (2004). Enhanced generation of intracellular Abeta42 amyloid peptide by mutation of presenilins PS1 and PS2. *Eur J Neurosci* **19**: 258–264.
6. Misonou, H, Morishima-Kawashima, M and Ihara, Y (2000). Oxidative stress induces intracellular accumulation of amyloid beta-protein (Abeta) in human neuroblastoma cells. *Biochemistry* **39**: 6951–6959.
7. Levites, Y, Jansen, K, Smithson, LA, Dakin, R, Holloway, VM, Das, P *et al.* (2006). Intracranial adeno-associated virus-mediated delivery of anti-pan amyloid beta, amyloid beta40, and amyloid beta42 single-chain variable fragments attenuates plaque pathology in amyloid precursor protein mice. *J Neurosci* **26**: 11923–11928.
8. Holliger, P and Hudson, PJ (2005). Engineered antibody fragments and the rise of single domains. *Nat Biotechnol* **23**: 1126–1136.
9. Zhu, Q, Zeng, C, Huhalov, A, Yao, J, Turi, TG, Danley, D *et al.* (1999). Extended half-life and elevated steady-state level of a single-chain Fv intrabody are critical for specific intracellular retargeting of its antigen, caspase-7. *J Immunol Methods* **231**: 207–222.
10. Lobato, MN and Rabbitts, TH (2003). Intracellular antibodies and challenges facing their use as therapeutic agents. *Trends Mol Med* **9**: 390–396.
11. Richardson, JH and Marasco, WA (1995). Intracellular antibodies: development and therapeutic potential. *Trends Biotechnol* **13**: 306–310.
12. Miller, TW and Messer, A (2005). Intrabody applications in neurological disorders: progress and future prospects. *Mol Ther* **12**: 394–401.
13. Fukuchi, K, Kamino, K, Deeb, SS, Furlong, CE, Sundstrom, JA, Smith, AC *et al.* (1992). Expression of a carboxy-terminal region of the beta-amyloid precursor protein in a heterogeneous culture of neuroblastoma cells: evidence for altered processing and selective neurotoxicity. *Brain Res Mol Brain Res* **16**: 37–46.
14. Strathdee, CA, McLeod, MR and Hall, JR (1999). Efficient control of tetracycline-responsive gene expression from an autoregulated bi-directional expression vector. *Gene* **229**: 21–29.
15. Cook, DG, Forman, MS, Sung, JC, Leight, S, Kolson, DL, Iwatsubo, T *et al.* (1997). Alzheimer's A beta(1-42) is generated in the endoplasmic reticulum/intermediate compartment of NT2N cells. *Nat Med* **3**: 1021–1023.

16. Hare, JF (2006). Intracellular pathways of folded and misfolded amyloid precursor protein degradation. *Arch Biochem Biophys* **451**: 79–90.
17. Selkoe, DJ (1997). Alzheimer's disease: genotypes, phenotypes, and treatments. *Science* **275**: 630–631.
18. Selkoe, DJ (1998). The cell biology of beta-amyloid precursor protein and presenilin in Alzheimer's disease. *Trends Cell Biol* **8**: 447–453.
19. Wisniewski, T, Ghiso, J and Frangione, B (1997). Biology of A beta amyloid in Alzheimer's disease. *Neurobiol Dis* **4**: 313–328.
20. Younkin, SG (1998). The role of A beta 42 in Alzheimer's disease. *J Physiol Paris* **92**: 289–292.
21. Oddo, S, Caccamo, A, Kitazawa, M, Tseng, BP and LaFerla, FM (2003). Amyloid deposition precedes tangle formation in a triple transgenic model of Alzheimer's disease. *Neurobiol Aging* **24**: 1063–1070.
22. Oddo, S, Caccamo, A, Shepherd, JD, Murphy, MP, Golde, TE, Kayed, R *et al.* (2003). Triple-transgenic model of Alzheimer's disease with plaques and tangles: intracellular Abeta and synaptic dysfunction. *Neuron* **39**: 409–421.
23. Mastrangelo, MA and Bowers, WJ (2008). Detailed immunohistochemical characterization of temporal and spatial progression of Alzheimer's disease-related pathologies in male triple-transgenic mice. *BMC Neurosci* **9**: 81.
24. Billings, LM, Oddo, S, Green, KN, McGaugh, JL and LaFerla, FM (2005). Intraneuronal Abeta causes the onset of early Alzheimer's disease-related cognitive deficits in transgenic mice. *Neuron* **45**: 675–688.
25. Hoe, HS and Rebeck, GW (2008). Functional interactions of APP with the apoE receptor family. *J Neurochem* **106**: 2263–2271.
26. Frazer, ME, Hughes, JE, Mastrangelo, MA, Tibbens, JL, Federoff, HJ and Bowers, WJ (2008). Reduced pathology and improved behavioral performance in Alzheimer's disease mice vaccinated with HSV amplicons expressing amyloid-beta and interleukin-4. *Mol Ther* **16**: 845–853.
27. Oddo, S, Billings, L, Kesslak, JP, Cribbs, DH and LaFerla, FM (2004). Abeta immunotherapy leads to clearance of early, but not late, hyperphosphorylated tau aggregates via the proteasome. *Neuron* **43**: 321–332.
28. Oddo, S, Caccamo, A, Tran, L, Lambert, MP, Glabe, CG, Klein, WL *et al.* (2006). Temporal profile of amyloid-beta (Abeta) oligomerization in an in vivo model of Alzheimer disease. A link between Abeta and tau pathology. *J Biol Chem* **281**: 1599–1604.
29. Fukuchi, K, Accavitti-Loper, MA, Kim, HD, Tahara, K, Cao, Y, Lewis, TL *et al.* (2006). Amelioration of amyloid load by anti-Abeta single-chain antibody in Alzheimer mouse model. *Biochem Biophys Res Commun* **344**: 79–86.
30. Fukuchi, K, Tahara, K, Kim, HD, Maxwell, JA, Lewis, TL, Accavitti-Loper, MA *et al.* (2006). Anti-Abeta single-chain antibody delivery via adeno-associated virus for treatment of Alzheimer's disease. *Neurobiol Dis* **23**: 502–511.
31. Lecerf, JM, Shirley, TL, Zhu, Q, Kazantsev, A, Amersdorfer, P, Housman, DE *et al.* (2001). Human single-chain Fv intrabodies counteract in situ huntingtin aggregation in cellular models of Huntington's disease. *Proc Natl Acad Sci USA* **98**: 4764–4769.
32. Paganetti, P, Calanca, V, Galli, C, Stefani, M and Molinari, M (2005). beta-site specific intrabodies to decrease and prevent generation of Alzheimer's Abeta peptide. *J Cell Biol* **168**: 863–868.
33. Lynch, SM, Zhou, C and Messer, A (2008). An scFv intrabody against the nonamyloid component of alpha-synuclein reduces intracellular aggregation and toxicity. *J Mol Biol* **377**: 136–147.
34. Skovronsky, DM, Doms, RW and Lee, VM (1998). Detection of a novel intraneuronal pool of insoluble amyloid beta protein that accumulates with time in culture. *J Cell Biol* **141**: 1031–1039.
35. Cardinale, A, Filesi, I, Mattei, S and Biocca, S (2003). Evidence for proteasome dysfunction in cytotoxicity mediated by anti-Ras intracellular antibodies. *Eur J Biochem* **270**: 3389–3397.
36. Shumway, SD, Maki, M and Miyamoto, S (1999). The PEST domain of IkappaBalpha is necessary and sufficient for in vitro degradation by mu-calpain. *J Biol Chem* **274**: 30874–30881.
37. Johnston, J, Tazelaar, J, Rivera, VM, Clackson, T, Gao, GP and Wilson, JM (2003). Regulated expression of erythropoietin from an AAV vector safely improves the anemia of beta-thalassemia in a mouse model. *Mol Ther* **7**: 493–497.
38. Haberman, RP and McCown, TJ (2002). Regulation of gene expression in adeno-associated virus vectors in the brain. *Methods* **28**: 219–226.
39. Bobo, RH, Laske, DW, Akbasak, A, Morrison, PF, Dedrick, RL and Oldfield, EH (1994). Convection-enhanced delivery of macromolecules in the brain. *Proc Natl Acad Sci USA* **91**: 2076–2080.
40. Lidar, Z, Mardor, Y, Jonas, T, Pfeffer, R, Faibel, M, Nass, D *et al.* (2004). Convection-enhanced delivery of paclitaxel for the treatment of recurrent malignant glioma: a phase I/II clinical study. *J Neurosurg* **100**: 472–479.
41. Kunwar, S (2003). Convection enhanced delivery of IL13-PE38QQR for treatment of recurrent malignant glioma: presentation of interim findings from ongoing phase 1 studies. *Acta Neurochir Suppl* **88**: 105–111.
42. Fiandaca, MS, Varenika, V, Eberling, J, McKnight, T, Bringas, J, Pivirotto, P *et al.* (2008). Real-time MR imaging of adeno-associated viral vector delivery to the primate brain. *Neuroimage*. (epub a head of print).
43. Janelsins, MC, Mastrangelo, MA, Park, KM, Sudol, KL, Narrow, WC, Oddo, S *et al.* (2008). Chronic neuron-specific tumor necrosis factor-alpha expression enhances the local inflammatory environment ultimately leading to neuronal death in 3xTg-AD mice. *Am J Pathol* **173**: 1768–1782.
44. Urabe, M, Ding, C and Kotin, RM (2002). Insect cells as a factory to produce adeno-associated virus type 2 vectors. *Hum Gene Ther* **13**: 1935–1943.
45. Wuertzer, CA, Sullivan, MA, Qiu, X and Federoff, HJ (2008). CNS delivery of vectored prion-specific single-chain antibodies delays disease onset. *Mol Ther* **16**: 481–486.
46. Janelsins, MC, Mastrangelo, MA, Oddo, S, LaFerla, FM, Federoff, HJ and Bowers, WJ (2005). Early correlation of microglial activation with enhanced tumor necrosis factor-alpha and monocyte chemoattractant protein-1 expression specifically within the entorhinal cortex of triple transgenic Alzheimer's disease mice. *J Neuroinflammation* **2**: 23.